JOURNAL OF CATALYSIS **162,** 104–117 (1996)
ARTICLE NO. 0264

# Oxidation of Volatile Organic Compounds on $Al_2O_3$, $Pd/Al_2O_3$, and $PdO/Al_2O_3$ Catalysts

Eric M. Cordi and John L. Falconer[1]

*Department of Chemical Engineering, University of Colorado, Boulder, Colorado 80309-0424*

Received December 4, 1995; revised April 29, 1996; accepted May 1, 1996

**Temperature-programmed desorption (TPD) and oxidation (TPO) were used to study the decomposition and oxidation of methanol, ethanol, acetaldehyde, formic acid, and acetic acid on $Al_2O_3$, $Pd/Al_2O_3$, and $PdO/Al_2O_3$ catalysts. The oxidation and decomposition rates were much higher on $Pd/Al_2O_3$ than on $Al_2O_3$, even though the volatile organic compounds (VOCs) were adsorbed on the $Al_2O_3$ support in both cases. The VOCs surface-diffused to Pd and mostly dehydrogenated during TPD whereas they oxidized to $CO_2$ and $H_2O$ in the presence of oxygen. Partial oxidation products also apparently formed on the surface during TPO and they oxidized completely above 550 K. Above 600 K, VOCs oxidation was consistent with the Mars–van Krevelen mechanism, involving the oxidation and reduction of Pd and PdO. On $PdO/Al_2O_3$ adsorbed VOCs were oxidized by lattice oxygen from PdO, but PdO was less active than Pd metal for VOC decomposition. Oxidation began at the same temperatures on $PdO/Al_2O_3$ whether or not $O_2$ was present, indicating that extraction of lattice oxygen from PdO was the limiting factor initially. After lattice oxygen was removed, metallic Pd decomposed VOCs and also adsorbed $O_2$, which was incorporated into the Pd lattice above 600 K. The reduction of PdO during TPD resulted in an autocatalytic oxidation since metallic Pd was more active than PdO. A portion of the VOCs reacted in parallel on $Al_2O_3$ since these sites are active for dehydration and dehydrogenation at moderate to high temperatures.** 

## INTRODUCTION

Volatile organic compounds (VOCs) are emitted in dilute concentrations from many industrial processes and internal combustion engines, and control of VOC emissions is often accomplished by thermal incineration to $CO_2$ and $H_2O$. Catalytic incineration can achieve conversions of greater than 99% while operating at a lower temperature (673 to 773 K) than a thermal incinerator (973 to 1473 K). The reduced operating temperature also means less auxiliary fuel is needed to preheat the waste stream and the reactor.

A review by Spivey (1) indicated that a majority of the research on deep catalytic oxidation lacks information about the surface reaction processes and kinetics. Instead, most research has focused on measurements of conversion as a function of temperature and catalyst composition. The improvement of catalysts for air pollution control can benefit from a fundamental knowledge of the catalytic surface processes. Thus, this study concentrates on transient measurements of decomposition and oxidation of methanol ($CH_3OH$), ethanol ($C_2H_5OH$), acetaldehyde ($C_2H_4O$), formic acid (HCOOH), and acetic acid ($CH_3COOH$) on $Pd/Al_2O_3$ catalysts. Alcohols and aldehydes are common pollutants, and methanol and ethanol are used in gasoline and as industrial solvents. Alcohol engines emit unburned methanol and ethanol plus formaldehyde and acetaldehyde as partial oxidation products. Finally, formic acid and acetic acid are partial oxidation products of the alcohols and aldehydes. Because CO is a product of decomposition of most of these VOCs, its oxidation was also studied.

We used temperature-programmed desorption (TPD) and oxidation (TPO) to study oxidation of the five VOCs, which adsorb on $Al_2O_3$ at room temperature. These transient methods enabled us to study oxidation and decomposition processes and to follow the oxidation state of the supported Pd metal. Both $Al_2O_3$ and $Pd/Al_2O_3$ were studied to examine the role of Pd in the oxidation and decomposition of VOCs adsorbed on $Al_2O_3$. Since PdO formed above 600 K during TPO of $Pd/Al_2O_3$, reactions were studied on $PdO/Al_2O_3$ to clarify the role of lattice oxygen in VOC oxidation.

## EXPERIMENTAL METHODS

Temperature-programmed desorption and oxidation experiments were performed on $Al_2O_3$, $Pd/Al_2O_3$, and $PdO/Al_2O_3$ in a flow system at atmospheric pressure. This system is similar to that described previously (2). Volatile organic compounds and CO were adsorbed on the catalyst at room temperature in He flow, and the catalyst temperature was then raised at a rate of 1 K/s in a He flow during TPD. For some TPO experiments, products formed at room temperature so the catalyst was first cooled to 223 K with liquid nitrogen vapor. The flow gas was then switched from

[1] E-mail: john.falconer@colorado.edu.



0021-9517/96 $18.00

He to 3% $O_2$/1% Ar/96% He and the catalyst temperature was raised at a rate of 1 K/s. The catalyst sample (25 mg, 60–80 mesh) was heated in a 1 cm o.d. tubular quartz reactor by a temperature-programmed electric furnace. A 0.5 mm o.d. chromel–alumel thermocouple, placed in the center of the catalyst bed, measured catalyst temperature and provided feedback to the temperature programmer. The effluent from the reactor was analyzed by a Balzers QMG 421C quadrupole mass spectrometer, which used a capillary inlet system for sampling and computer acquisition for detection of multiple mass peaks.

Volatile organic compounds were adsorbed by injecting 0.5-ml liquid samples into the He flow stream. The liquid evaporated from the side of the quartz reactor, and thus only vapor contacted the catalyst bed. Carbon monoxide ($^{12}CO$ and $^{13}CO$) was adsorbed by injecting 0.15 $cm^3$ (STP) pulses of a 10% $^{12}CO$/He mixture or 0.05 $cm^3$ (STP) pulses of pure $^{13}CO$ twice each minute for a 30-min period. Coadsorption experiments were performed both with the $^{13}CO$ and with the VOC adsorbed first.

In some experiments, interrupted TPO was used. After $CH_3OH$ or $C_2H_5OH$ was adsorbed, the catalyst temperature was raised in 3% $O_2$ (TPO) to 573 K and the sample was then rapidly cooled (at a rate of approximately 50 K/s). The inlet gas was then switched to He at room temperature and TPD was carried out to 773 K. This procedure helped determine what species remained on the surface when oxidation was only partially complete.

During TPD and TPO numerous mass peaks were monitored to be sure all products were detected. Corrections for cracking in the mass spectrometer were made for each product, and for some species multiple corrections were necessary. Each species was calibrated by injecting a measured amount into the flow gas stream between the reactor and mass spectrometer. Note that the $H_2O$ product that formed during TPO (and during TPD in some cases) is not shown in the figures so that the other products are easier to distinguish. Since $H_2O$ readsorbs on the $Al_2O_3$ support, its appearance in the gas phase is limited by desorption, and thus the $H_2O$ spectra provide no additional information about the reaction processes. In addition, $H_2O$ calibrations are less accurate. Only the fact that $H_2O$ is a reaction product is of interest.

The 3.7% $Pd/Al_2O_3$ catalyst was prepared by impregnating Kaiser A-201 $Al_2O_3$ incipient wetness with an aqueous solution of $PdCl_2$ (3). The impregnated $Al_2O_3$ was air dried for 24 h and then dried in vacuum at 373–383 K for 24 h. The catalyst was then calcined for 10 min at 573 K, reduced at 573 K for 5 h, and then passivated in 2% $O_2/N_2$ at 300 K. Finally, the $Pd/Al_2O_3$ was reduced again at 773 K in $H_2$ for 5 h. The Pd weight loading was measured by inductively coupled plasma mass spectroscopy (ICP).

The $Al_2O_3$ was pretreated in 3% $O_2$ at 873 K for 10 min before each experiment to dehydrate it and to oxidize contaminants on the surface. The $Pd/Al_2O_3$ catalyst was pretreated by oxidation in 3% $O_2$ at 773 K for 30 min. When a $PdO/Al_2O_3$ sample was desired, this was the only pretreatment necessary. To obtain $Pd/Al_2O_3$, the sample was then reduced in $H_2$ flow at 573 K for 30 min, the flow was switched to He at 573 K, and the temperature was slowly raised to 773 K and held there 10 min to remove $H_2$ and $H_2O$ from the catalyst. The oxygen treatment redispersed the Pd on the surface, and low-temperature reduction prevented sintering, which occurs above 573 K in $H_2$ (4).

Exothermic oxidation of VOCs can potentially create significant temperature gradients in the catalyst particles and the reactor. To minimize these effects, small catalyst samples were used (25 mg) so that the total heat generated was small, and high gas flow rates (100 $cm^3$/min (STP)) were used to allow rapid heat removal. Reactions were also run in 3% $O_2$ since rates increase with $O_2$ concentration, and less-than-saturation amounts of VOCs were used to limit the total heat generated. For 3.7% Pd loading under these conditions, the temperature gradients internal and external to the catalyst particles were small (5, 6). In contrast, for 100 mg of 9% $Pd/Al_2O_3$ catalyst at saturation coverage of $CH_3OH$, the heat released in 3% $O_2$ due to oxidation caused the catalyst temperature to rise at a rate much faster than 1 K/s. For the 3% Pd loading and the conditions used in this study, mass transfer limitations were negligible based on the analysis by Demmin and Gorte (7).

## RESULTS

### *Temperature-Programmed Desorption*

*Alumina.* As shown in Fig. 1a, methanol decomposed on alumina due to both dehydrogenation and dehydration (8). Most of the methanol dehydrogenated to CO and $H_2$ between 600 and 900 K. The $H_2/(CO + CO_2)$ ratio was 1.9. Less than 40% of the adsorbed methanol dehydrated, at a much lower temperature than dehydrogenation, to form dimethyl ether and water. A small amount of $CO_2$ was seen above 700 K, and some unreacted methanol desorbed over a broad temperature range. For ethanol, dehydration to ethylene and water was the dominant decomposition pathway during TPD on alumina (Fig. 1b), and ethylene formed in a peak at 640 K. Simultaneously, dehydrogenation formed acetaldehyde and $H_2$, but three times as much $H_2$ desorbed as acetaldehyde. The remaining acetaldehyde probably remained on the surface and further dehydrogenated to form a carboneous species. A small amount of $CO_2$ was seen above 800 K, and this may be from acetaldehyde decomposition; as shown below, acetaldehyde decomposed slowly on alumina. Approximately one-third of the original carbon in ethanol remained on the surface at 873 K.

Acetaldehyde was the least reactive compound studied on alumina. The only gas-phase products were CO, $CO_2$,

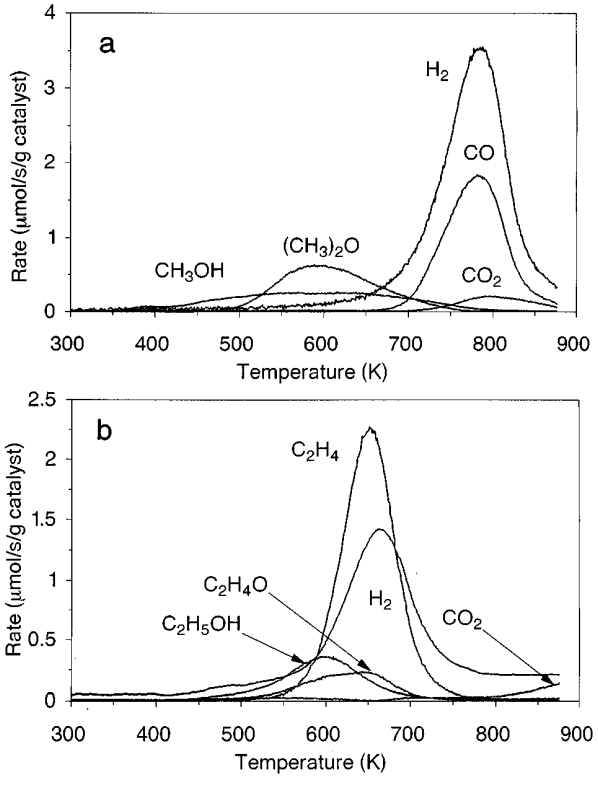


**FIG. 1.** Temperature-programmed desorption spectra of $CH_3OH$ (a) and $C_2H_5OH$ (b) adsorbed on $Al_2O_3$.

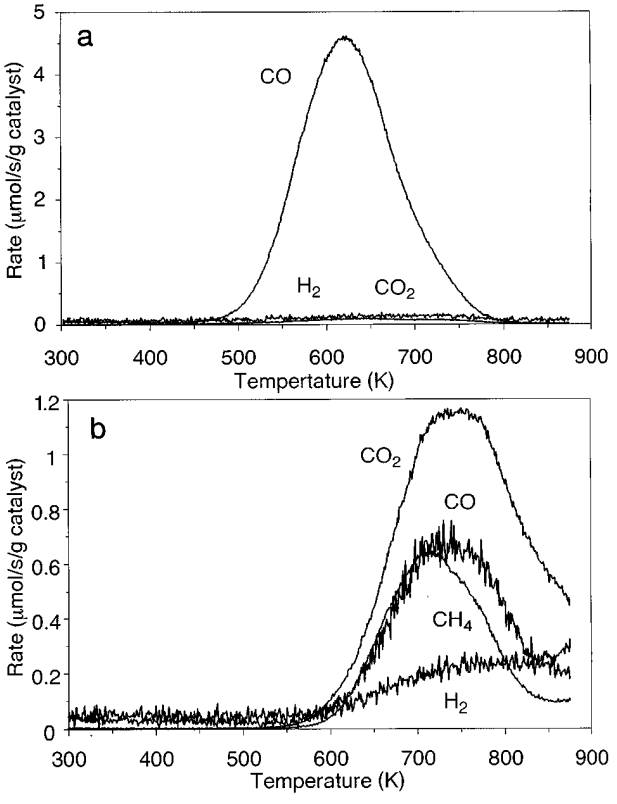


**FIG. 3.** Temperature-programmed desorption spectra of HCOOH (a) and $CH_3COOH$ (b) adsorbed on $Al_2O_3$.

and $H_2$. Decomposition began at 450 K and was not complete at 973 K, as shown in Fig. 2. More than two-thirds of the carbon in acetaldehyde remained on the surface, probably as a reaction product. A subsequent TPO converted the remaining species adsorbed on the alumina to CO, $CO_2$, and $H_2O$.

Formic acid dehydrated almost completely to CO and $H_2O$, and the CO formed in a peak at 620 K (Fig. 3a). Less than 4% of the adsorbed formic acid dehydrogenated to $CO_2$ and $H_2$ in the same temperature range in which CO formed. No unreacted HCOOH desorbed. Acetic acid decomposed much slower on alumina than formic acid did, and as shown in Fig. 3b the reaction was not complete at 873 K. The carbon–carbon bond was cleaved to form CO and $CO_2$ from the $\alpha$-carbon, and some of the resulting $CH_3$ groups were hydrogenated to $CH_4$. The $CH_4$ amount was much smaller than the CO-plus-$CO_2$ amounts, however, and the rest of the $\beta$-carbon remained on the surface. The increasing rate of $H_2$ formation up to 873 K most likely corresponds to continued dehydrogenation of $CH_3$ to surface carbon and hydrogen. Approximately 60% of the adsorbed acetic acid reacted by 873 K.

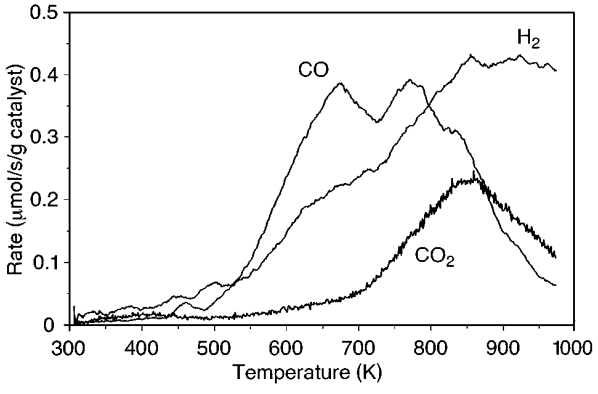


**FIG. 2.** Temperature-programmed desorption spectra of $C_2H_4O$ adsorbed on $Al_2O_3$.

*Palladium/alumina.* The addition of palladium to alumina dramatically lowers the temperature for VOC decomposition and for some VOCs also changes the product distribution. The alumina surface area (200 $m^2/g$ (9)) is much larger than the Pd surface area (3.3 $m^2/g$, calculated from CO adsorption), and the amount of adsorption did not change significantly from that on alumina alone, so it appears that almost all the adsorption is on the alumina. Previous studies on $Ni/Al_2O_3$ catalysts showed that neither methanol nor ethanol adsorbed to a significant extent on the Ni surface at room temperature, at least in the presence of $H_2$ (8). In contrast, some HCOOH adsorbed on the Ni surface.

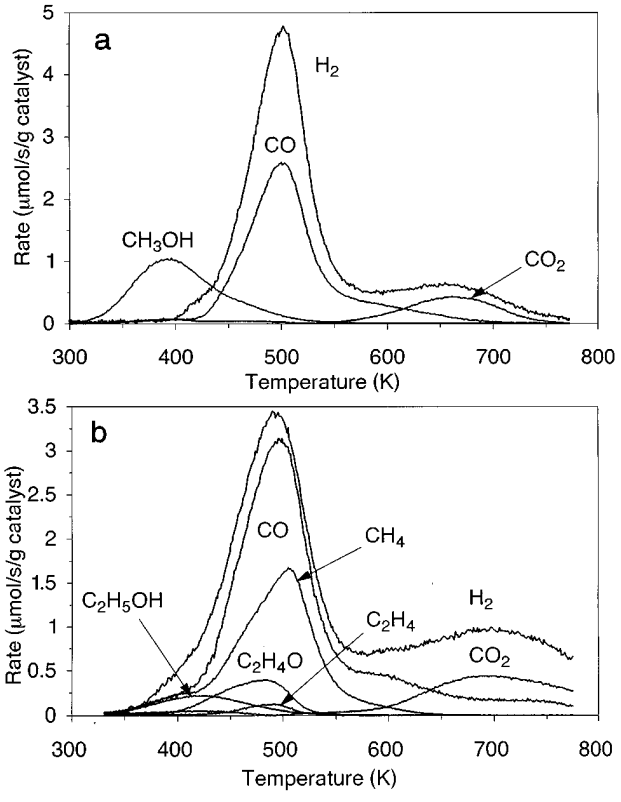


**FIG. 4.** Temperature-programmed desorption spectra of $CH_3OH$ (a) and $C_2H_5OH$ (b) adsorbed on $Pd/Al_2O_3$.

On $Pd/Al_2O_3$, methanol dehydrogenated to form CO and $H_2$ simultaneously in peaks at 500 K, which is 280 K lower than on alumina. As shown in Fig. 4a, unreacted methanol and small amounts of $CO_2$ were the only other products. No dehydration to dimethyl ether was observed. The $H_2/(CO + CO_2)$ ratio is 2.0. On $Pd/Al_2O_3$, ethanol underwent CO elimination to form $CH_4$, CO, and $H_2$ as the main products, as shown in Fig. 4b. Experiments with isotope labeling on the $\alpha$-carbon showed that the $\alpha$-carbon formed CO and the $\beta$-carbon formed $CH_4$ (10). Small amounts of ethanol dehydrated to ethylene and dehydrogenated to acetaldehyde at the same temperature. Unreacted ethanol desorbed at a lower temperature than from alumina and in a smaller amount. Approximately half the original carbon in ethanol was detected as CO and half the original hydrogen was detected as $H_2$. Since less $CH_4$ formed than CO, some $\beta$-carbon and hydrogen remained on the catalyst during TPD.

Acetaldehyde started decomposing on $Pd/Al_2O_3$ above 350 K and the main products were CO and $H_2$, both of which formed in broad peaks up to 773 K. Twenty-one percent of the carbon in the adsorbed acetaldehyde desorbed as unreacted acetaldehyde, $CH_4$, and $CO_2$ in broad peaks. Reaction was not complete at 773 K, and approximately 20% of the adsorbed acetaldehyde had not formed gas-phase products by 773 K.

Formic acid decomposition changed from dehydration on alumina almost exclusively to mostly dehydrogenation on $Pd/Al_2O_3$, and the reaction was much faster than on alumina. As shown in Fig. 5a, $CO_2$ and $H_2$ started forming at 300 K and formed over a broad temperature range. About 15% of the formic acid dehydrated to CO and $H_2O$ between 420 and 720 K. In contrast to formic acid, the rate of acetic acid decomposition was increased less by the presence of palladium, but the product distribution changed to mostly dehydrogenation products. Carbon monoxide and $H_2$ were the main products, and the $H_2/(CO + CO_2)$ ratio was 0.93. As shown in Fig. 5b, only small amounts of $CO_2$ and $CH_4$ were seen, whereas $CO_2$ was the dominant product on alumina. About 85% of the carbon in adsorbed acetic acid had reacted and desorbed as gas-phase products by 773 K.

*Palladium oxide/alumina.* When palladium was oxidized, the temperature where decomposition began increased for all the VOCs, and more $CO_2$ and $H_2O$ formed as reaction products. As shown in Fig. 6a, when methanol decomposed during TPD on $PdO/Al_2O_3$, the starting temperatures and the peak temperatures for formation of CO and $H_2$ were higher than on $Pd/Al_2O_3$ (Fig. 4a). In addition, $CO_2$ and $H_2O$ started to form at the same temperature as CO. Apparently decomposition was slower on the oxide, and as CO and $H_2$ formed they were oxidized by lattice

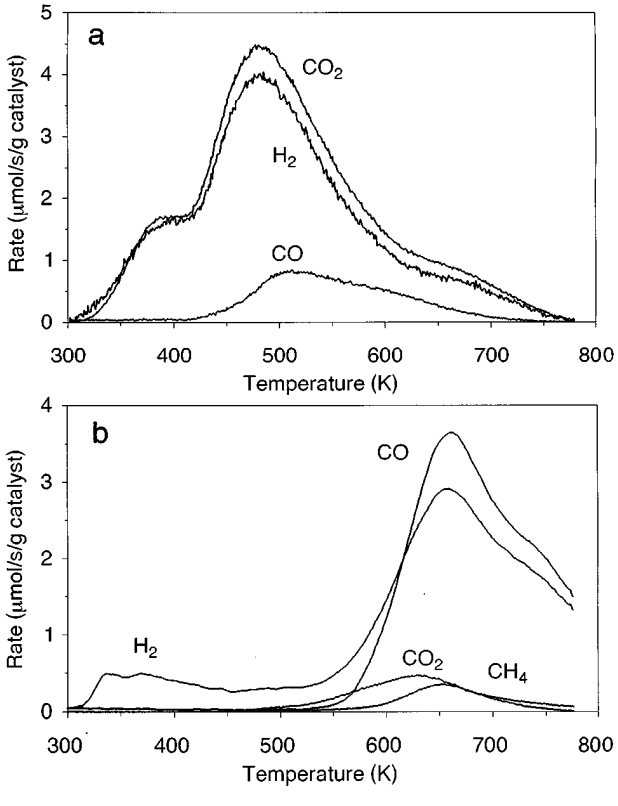


**FIG. 5.** Temperature-programmed desorption spectra of HCOOH (a) and $CH_3COOH$ (b) adsorbed on $Pd/Al_2O_3$.

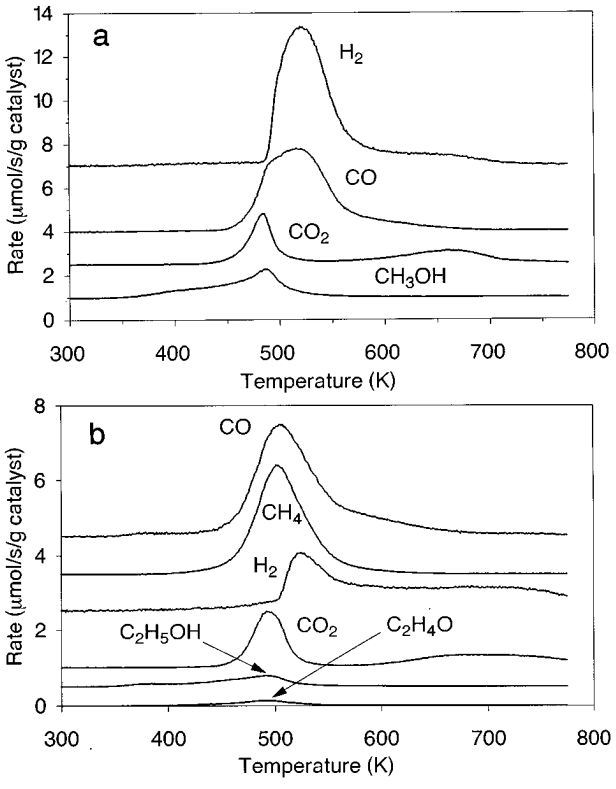


**FIG. 6.** Temperature-programmed desorption spectra of $CH_3OH$ (a) and $C_2H_5OH$ (b) adsorbed on $PdO/Al_2O_3$.

oxygen from PdO. As the lattice oxygen was consumed, $H_2$ and CO became the dominant products, as was observed on $Pd/Al_2O_3$. The appearance of $H_2$ was delayed relative to CO, apparently because adsorbed hydrogen was more readily oxidized than adsorbed CO. Thus on $PdO/Al_2O_3$ the dehydrogenation products were oxidized, and the reaction changed the catalyst composition. In addition to the $CO_2$ peak at 490 K, a second $CO_2$ peak formed simultaneously with $H_2$ at 670 K, as was seen on $Pd/Al_2O_3$.

Similar behavior was observed for ethanol decomposition on $PdO/Al_2O_3$. Carbon dioxide, CO, $CH_4$, and $H_2O$ formed initially, but at a higher temperature than that on $Pd/Al_2O_3$. As shown in Fig. 6b, $H_2$ exhibited the largest increase in initial temperature of formation. On $Pd/Al_2O_3$, $H_2$ started to form at 350 K, whereas on $PdO/Al_2O_3$, $H_2$ did not form until almost 500 K and did so in much smaller amounts. Most of the $H_2$ was oxidized by the lattice oxygen of PdO to form water. That is, the same CO elimination reaction that took place on $Pd/Al_2O_3$ was occurring on $PdO/Al_2O_3$, and the reaction products were then oxidized by the lattice oxygen. The $CH_4$ product appeared to be the least affected by palladium oxidation. The peaks were narrower than on $Pd/Al_2O_3$ because the initial rate was slower on PdO, but as the reaction proceeded and the lattice oxygen was removed, the more active Pd surface was exposed so that the reaction was autocatalytic. The $H_2$ and CO peaks were not identical because adsorbed hydrogen was oxidized faster than adsorbed CO. Less than 4% of the adsorbed ethanol dehydrogenated to acetaldehyde, which desorbed in a peak near 500 K. That is, there is no evidence of oxidative dehydrogenation of ethanol to acetaldehyde.

Acetaldehyde initially decomposed at a much slower rate on PdO than on Pd, but once reaction started $CO_2$ formed rapidly on PdO, as might be expected for an autocatalytic reaction. As seen in Fig. 7, $CO_2$ formed in a narrow peak at 530 K, and $H_2O$ and CO formed simultaneously. Above 570 K, mostly CO and $H_2$ formed, apparently after significant lattice oxygen had been extracted from PdO, and decomposition was incomplete when heating was stopped at 773 K; only 64% of the acetaldehyde had formed gas-phase products by 773 K.

Formic acid also decomposed at a slower rate on $PdO/Al_2O_3$ than on $Pd/Al_2O_3$. As shown in Fig. 8a, $CO_2$ did not start to form until 400 K on PdO versus 300 K on Pd. In addition, $CO_2$ and $H_2O$ were essentially the only products; only small amounts of $H_2$ and CO were seen. Since most of the formic acid on Pd dehydrogenates to $CO_2$ and $H_2$, not much CO was formed to extract lattice oxygen from PdO and almost all the hydrogen that formed was oxidized to water. The $CO_2$ peak is narrow in Fig. 8a, whereas it is much broader on Pd (Fig. 5a); the $CO_2$ peak is probably the result of an autocatalytic process as seen for some of the other VOCs. Acetic acid decomposed much slower than formic acid on PdO, but the $CO_2$ peak, which was at a higher temperature, was narrower (Fig. 8b) and is even more indicative of an autocatalytic process. Water also formed. After the $CO_2$ rate had decreased, $H_2$, CO, and $CH_4$ formed simultaneously with peak temperatures and shapes similar to the same products on Pd.

### *Temperature-Programmed Oxidation*

*Alumina.* Since alumina is not a good oxidation catalyst, the TPO spectra were similar to the TPD spectra for

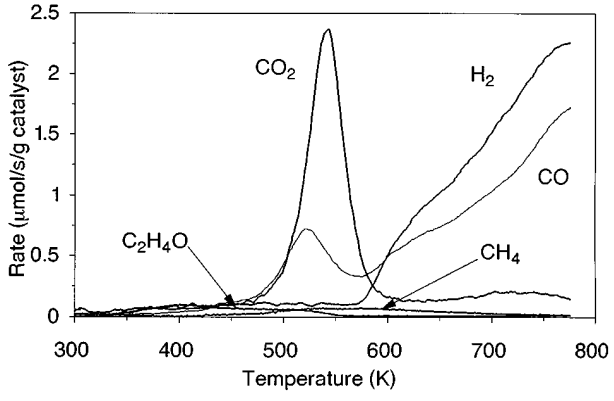


**FIG. 7.** Temperature-programmed desorption spectra of $C_2H_4O$ adsorbed on $PdO/Al_2O_3$.

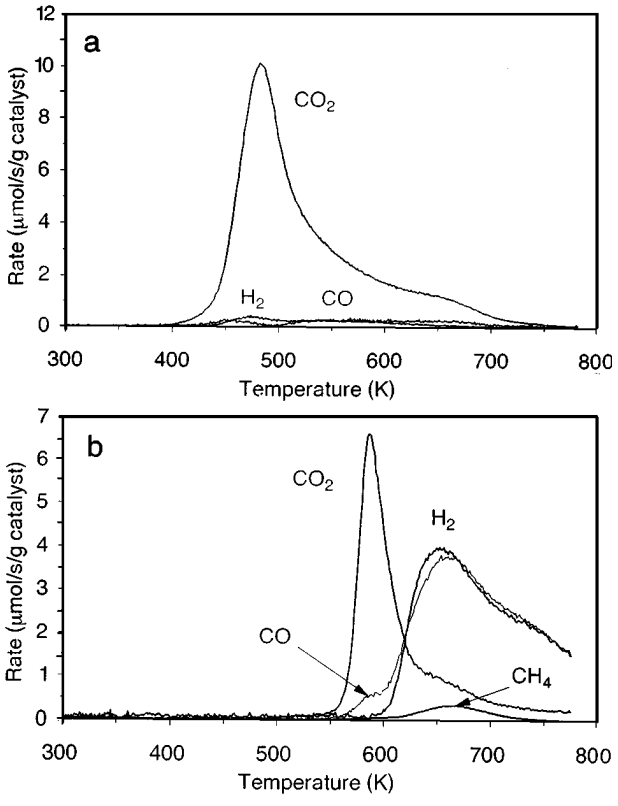


**FIG. 8.** Temperature-programmed desorption spectra of HCOOH (a) and $CH_3COOH$ (b) adsorbed on $PdO/Al_2O_3$.

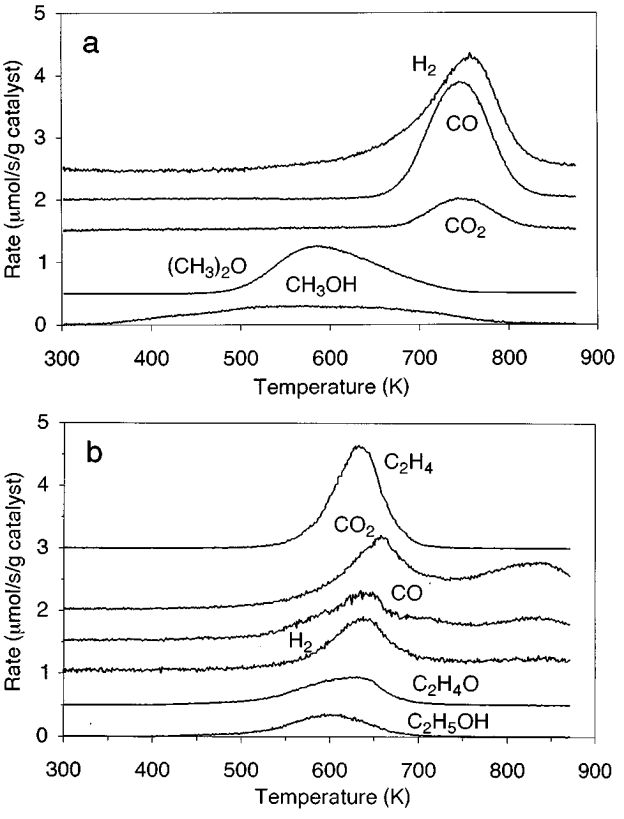


**FIG. 9.** Temperature-programmed oxidation spectra of $CH_3OH$ (a) and $C_2H_5OH$ (b) adsorbed on $Al_2O_3$.

each VOC, but some oxidation took place during TPO. For adsorbed methanol, the same products were observed, and at similar locations, during TPO (Fig. 9a) as during TPD (Fig. 1a). The dominant reaction was dehydrogenation to CO and $H_2$, which appeared in peaks near 750 K, which is 50 K lower than during TPD. The $H_2$ peak seen during TPO was half the size of that observed during TPD, and water formation increased correspondingly. The CO peak was about the same size during TPO and TPD, but twice as much $CO_2$ was seen during TPO, and the $CO_2$ peak was at 50 K lower temperature. Because the hydrogen was preferentially oxidized, the CO and $H_2$ peaks do not coincide.

The same products were observed from ethanol during TPO and TPD and they were also at similar temperatures, as shown in Fig. 9b. The amounts of ethylene and $H_2$ were approximately half of those observed during TPD, and much more $CO_2$ formed during TPO. Also, CO, $CO_2$, and $H_2$ formed at a higher rate at 873 K during TPO. The locations of the ethylene and unreacted ethanol peaks were unchanged from TPD, but 50% more acetaldehyde formed during TPO.

Because acetaldehyde was strongly adsorbed on alumina and decomposed only at higher temperature, more acetaldehyde was on the surface during TPO at high temperature where the oxidation rate was high. Thus, the maximum rates of $CO_2$ and CO formation were 6–10 times higher during TPO than during TPD. As shown in Fig. 10, $CO_2$ and CO were the main products; water also formed simultaneously with $CO_2$, whereas the $H_2$ signal was small.

Formic acid decomposed to mostly CO and $H_2O$ during TPO on alumina, and the spectra were almost identical to those for TPD and thus are not shown here. Only a small amount of $H_2$ and $CO_2$ formed; essentially none of the $H_2$ or CO products were oxidized on alumina. Likewise, TPO

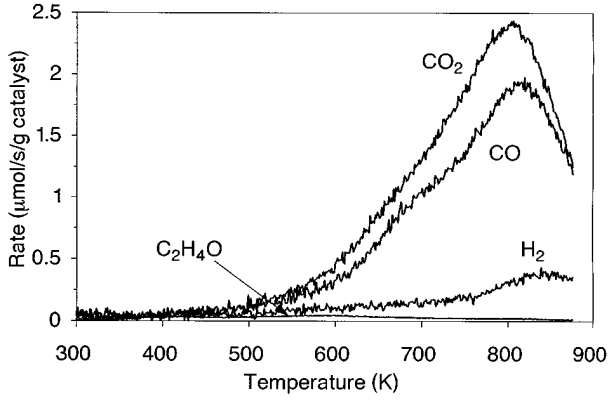


**FIG. 10.** Temperature-programmed oxidation spectra of $C_2H_4O$ adsorbed on $Al_2O_3$.

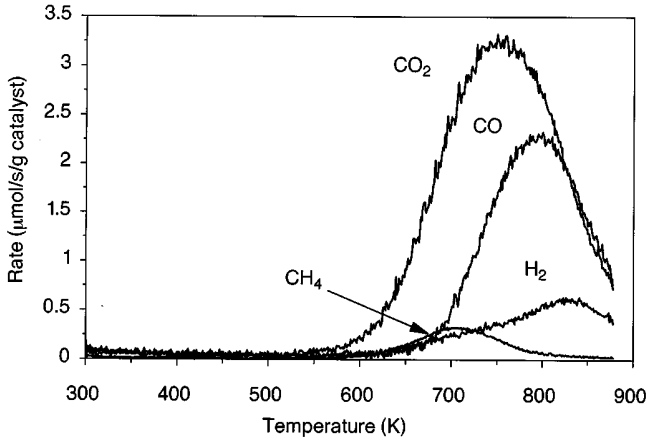


**FIG. 11.** Temperature-programmed oxidation spectra of $CH_3COOH$ adsorbed on $Al_2O_3$.

of acetic acid on alumina was similar to TPD. As shown in Fig. 11, mostly $CO_2$, CO, and $H_2O$ formed. About the same amount of $H_2$ desorbed during TPO and TPD, but only 30% as much $CH_4$ formed during TPO.

*Palladium/alumina.* On $Pd/Al_2O_3$, the TPO and TPD spectra were completely different. For all VOCs except acetic acid, reaction products started forming no later than 350 K, and the main products in all cases were $CO_2$ and $H_2O$. Only small amounts of gas-phase, partial oxidation products were observed.

Figure 12 shows that most of the adsorbed methanol oxidized to $CO_2$ (and $H_2O$) during TPO on $Pd/Al_2O_3$. Two aspects of the $CO_2$ spectrum are of interest: three distinct peaks (330, 500, and 620 K) were observed, and much of the $CO_2$ formed at a higher temperature than the methanol decomposition products seen during TPD. That is, most of the $CO_2$ formed at a slower rate during TPO than CO formed during TPD. Apparently a partial oxidation product formed at lower temperature and it oxidized more slowly than methanol decomposed. The only gas-phase, partial oxidation products were formaldehyde and CO in small amounts.

Ethanol oxidized on $Pd/Al_2O_3$ mostly to $CO_2$ and $H_2O$, though small amounts of acetaldehyde, CO, and unreacted ethanol were also observed when 0.5-$\mu$l ethanol was adsorbed. Two distinct $CO_2$ peaks were seen at 490 and 690 K, and the majority of $CO_2$ formed above 600 K. When a 0.1-$\mu$l sample was adsorbed, the two $CO_2$ peaks were at 450 and 730 K (Fig. 13a). The $CO_2$ spectra were similar for the two ethanol coverages except for the relative heights of the two $CO_2$ peaks. For the 0.5-$\mu$l sample, the peak-rate ratio of the two peaks (high temperature to low temperature) was about 1.5, whereas the ratio was 3.6 when 0.1 ml was adsorbed.

Acetaldehyde oxidized almost completely to $CO_2$ and $H_2O$ on $Pd/Al_2O_3$, as shown in Fig. 13b. Carbon dioxide formed in two peaks: the peak at 480 K was narrow (halfwidth of 60 K), whereas the peak at 700 K was broader, so the majority of the $CO_2$ formed above 550 K. Small amounts of $H_2$, CO, and acetaldehyde were seen.

Only $CO_2$ and $H_2O$ were observed for TPO of formic acid (Fig. 14a) and acetic acid (Fig. 14b). Carbon dioxide formed in two broad peaks from 300 to 700 K for formic acid oxidation, and the TPO spectra did not correspond to formic acid

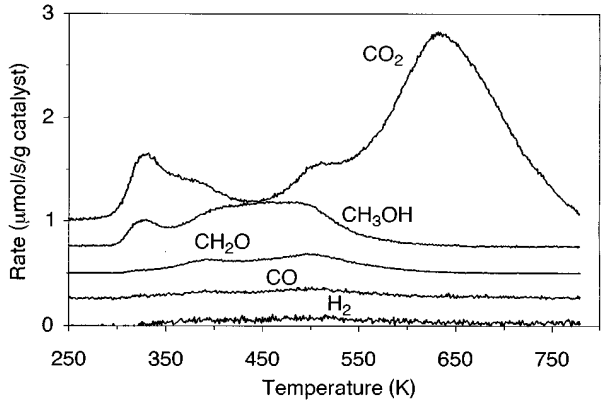


**FIG. 12.** Temperature-programmed oxidation spectra of $CH_3OH$ adsorbed on $Pd/Al_2O_3$.

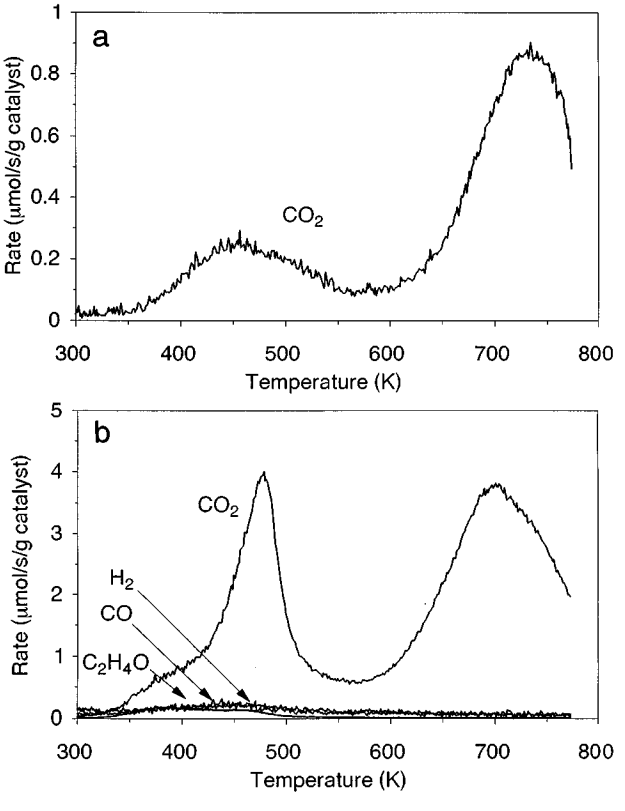


**FIG. 13.** Temperature-programmed oxidation spectra of $C_2H_5OH$ (a) and $C_2H_4O$ (b) adsorbed on $Pd/Al_2O_3$.

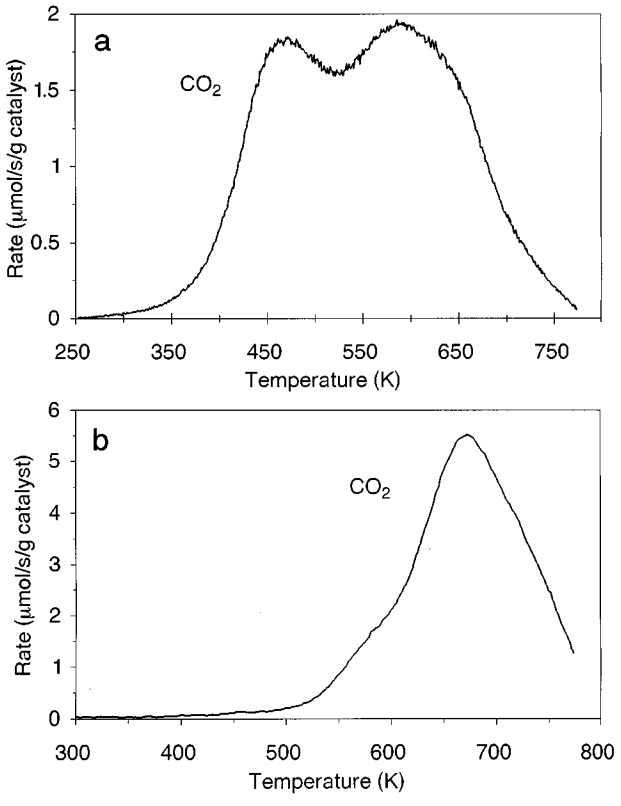


**FIG. 14.** Temperature-programmed oxidation spectra of HCOOH (a) and $CH_3COOH$ (b) adsorbed on $Pd/Al_2O_3$.

dehydrogenation and subsequent oxidation of the products. Acetic acid oxidized more slower than formic acid in a single $CO_2$ peak at 670 K, and the $CO_2$ peak was similar to the CO peak seen during TPD. During TPO, nearly all the adsorbed acetic acid had reacted by 773 K.

*Palladium oxide/alumina.* Oxidation of all the VOCs was slower on $PdO/Al_2O_3$ than on $Pd/Al_2O_3$ during TPO, and $CO_2$ started forming near 450 K instead of 350 K. The temperature for the onset of oxidation product formation was the same during TPO and TPD on $PdO/Al_2O_3$, as if oxygen had to be extracted from the PdO before significant oxidation could occur. In addition, more $CO_2$ formed above 600 K during TPO of methanol, ethanol, and acetaldehyde than $CO + CO_2$ formed above 600 K during TPD. Apparently a more stable oxidation product formed that did not oxidize or decompose as fast as the originally adsorbed species.

Most of the adsorbed methanol on $PdO/Al_2O_3$ oxidized to $CO_2$ and $H_2O$ during TPO. Carbon dioxide started forming at the same temperature as it formed during TPD on $PdO/Al_2O_3$, but much more $CO_2$ formed and it formed in two distinct peaks, as shown in Fig. 15. About 7% of the methanol was partially oxidized to formaldehyde, whereas less than 3% converted to formaldehyde during TPD. The amount of dimethyl ether doubled, and nearly

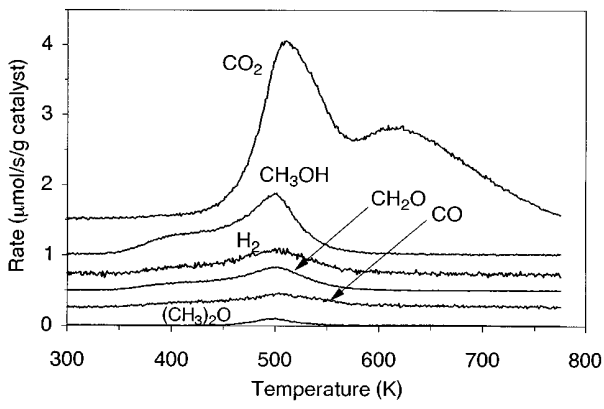


**FIG. 15.** Temperature-programmed oxidation spectra of $CH_3OH$ adsorbed on $PdO/Al_2O_3$.

equal amounts of unreacted methanol were seen during TPO and TPD.

Ethanol also oxidized to $CO_2$ in two distinct peaks on $PdO/Al_2O_3$ (Fig. 16a), and the main products were $CO_2$ and $H_2O$, both of which started forming at the same temperature during TPO and TPD. A 0.1-$\mu$l sample of ethanol was adsorbed to minimize heat transfer problems. Approximately 45% of the $CO_2$ formed above 600 K, whereas less than 18% of the carbon in ethanol was seen as a gas-phase

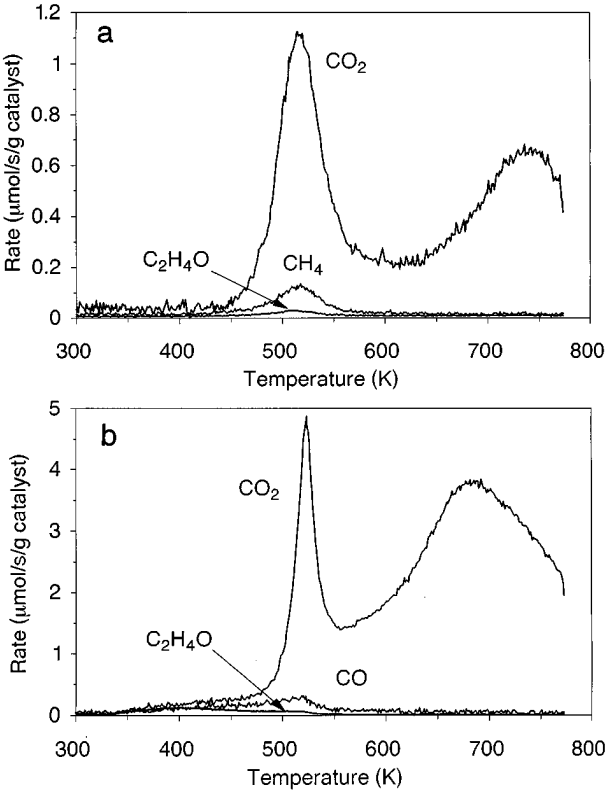


**FIG. 16.** Temperature-programmed oxidation spectra of $C_2H_5OH$ (a) and $C_2H_4O$ (b) adsorbed on $PdO/Al_2O_3$.

species above 600 K during TPD. A small amount of $CH_4$ and an even smaller amount of acetaldehyde formed with peaks near 510 K.

As shown in Fig. 16b, the $CO_2$ spectrum for acetaldehyde oxidation was similar to that for ethanol TPO. Carbon dioxide formed in two peaks; the 530 K peak was narrow and most of the $CO_2$ formed above 550 K in a broad peak. The 530 K peak started to form at the same temperature as $CO_2$ during TPD, but the peak was much narrower (20 K halfwidth) during TPO, as might be expected of an autocatalytic reaction. Water started to form at the same temperature as $CO_2$ and small amounts of acetaldehyde and CO were also seen.

Only $CO_2$ and $H_2O$ formed during TPO of formic acid and acetic acid on $PdO/Al_2O_3$, and formic acid oxidized much more rapidly. Similarly, formic acid decomposed during TPD more rapidly than did acetic acid. For formic acid, $CO_2$ formed in a broader peak during TPO, as shown in Fig. 17a, and its formation started at the same temperature as it did during TPD. The single $CO_2$ peak at 690 K from acetic acid oxidation (Fig. 17b) was 100 K higher than the $CO_2$ peak from TPD, and it was also broader.

*Carbon monoxide on palladium.* Carbon monoxide only adsorbed on the Pd surface of $Pd/Al_2O_3$, and because CO oxidation is rapid on Pd, TPO was started at 223 K.

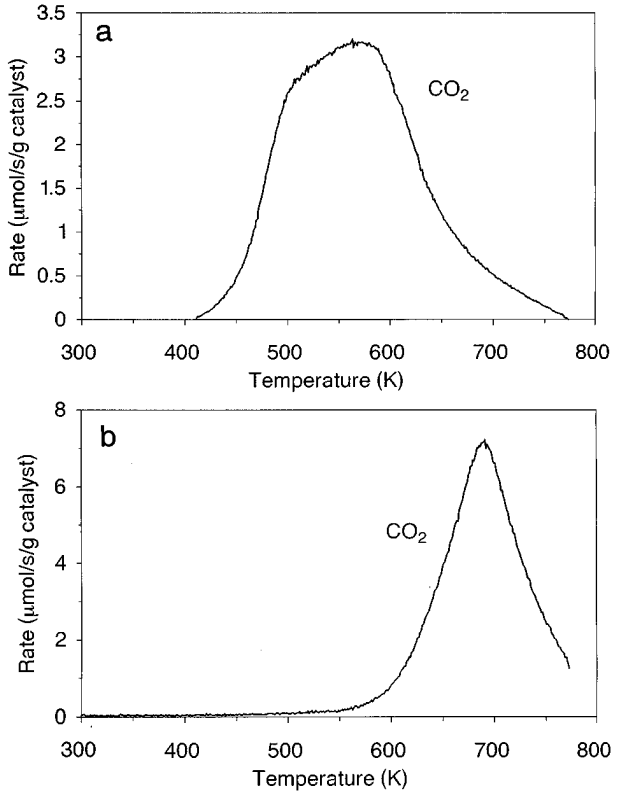


**FIG. 17.** Temperature-programmed oxidation spectra of HCOOH (a) and $CH_3COOH$ (b) adsorbed on $PdO/Al_2O_3$.

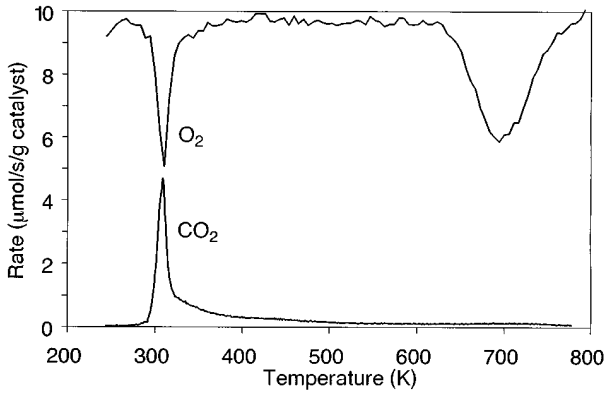


**FIG. 18.** Temperature-programmed oxidation spectra of CO adsorbed at 300 K on $Pd/Al_2O_3$.

As shown in Fig. 18, $CO_2$ started to form at 270 K in a narrow peak (15 K halfwidth) centered at 310 K, and $CO_2$ continued to form in a high-temperature tail. No unreacted CO desorbed during TPO. Oxygen consumption coincided with $CO_2$ formation and the amount of $O_2$ consumed below 400 K was equal to the total $CO_2$ produced. That is, the overall reaction is:

$$CO(a) + O_2(g) \rightarrow CO_2(g) + O(a)$$

Additional $O_2$ uptake was observed above 600 K with a maximum at 690 K. Since the identical $O_2$ uptake was seen above 600 K on a fresh $Pd/Al_2O_3$ catalyst, this uptake was attributed to Pd oxidation. Approximately 0.8 mol of oxygen atoms were consumed per mol of Pd; a more precise ratio was difficult to obtain because of noise in the oxygen signal. No additional $O_2$ uptake was observed during a repeat TPO on an oxidized sample. Freshly reduced $Pd/Al_2O_3$ was black, but after TPO to 773 K the sample turned a yellowish-brown. The same color change was observed by Garbowski *et al.* (11) and Albers *et al.* (12) during Pd oxidation.

Carbon monoxide also adsorbed on PdO, and its coverage was approximately the same as that on $Pd/Al_2O_3$. Adsorbed CO was oxidized on PdO during TPD and the main product was $CO_2$, as shown in Fig. 19a; only 10% of adsorbed CO desorbed unreacted. Carbon dioxide started forming at just about 300 K in several overlapping peaks, with a narrow peak centered at 510 K. This was the same temperature where lattice oxygen was extracted from PdO by adsorbed VOCs and is indicative of an autocatalytic reaction. Similarly, during TPO, $CO_2$ started forming just above 300 K, had a broad maximum around 400 K, and as shown in Fig. 19b, $CO_2$ continued to form until 773 K, but a narrow peak was not present as in TPD. Ten percent less $CO_2$ formed than was observed during TPO on $Pd/Al_2O_3$.

Methanol and $^{13}CO$ were coadsorbed on $Pd/Al_2O_3$ at 223 K and TPO was carried out. The $^{13}CO_2$ from $^{13}CO$ oxidation starting forming below 300 K, whereas $CO_2$ pro-

duction from methanol oxidation was slow until 400 K, when $^{13}CO_2$ production was ending. Above 400 K the $CO_2$ production was identical to that observed for methanol oxidation alone on $Pd/Al_2O_3$. The spectra did not depend on which reactant was adsorbed first, and there appeared to be little interaction between the absorbed species. The $^{13}CO$ was adsorbed on the Pd and the methanol on the alumina.

*Interrupted TPO.* Temperature-programmed oxidations of methanol and ethanol were interrupted at 573 K and the catalyst was cooled to room temperature before TPD was carried out. As shown in Fig. 20a for adsorbed methanol, $CO_2$, $H_2$, and CO formed during TPD; water also desorbed. Carbon dioxide formed first, above 500 K, but $H_2$ and CO did not form in significant quantities until above 573 K. The $H_2/(CO) + CO_2)$ ratio above 573 K was approximately 1.0. During TPD following interrupted TPO for adsorbed ethanol, $H_2$, CO, $CO_2$, $CH_4$, and $H_2O$ formed as shown in Fig. 20b. Some products were still on the surface at 773 K, since the signals had not reached zero at 773 K. The ratio of $H_2/(CO + CO_2)$ was approximately 1.0 above 600 K. The TPD for both methanol and ethanol exhibited a narrow $CO_2$ peak near 573 K that may have been due to reaction of oxygen that adsorbed on the palladium as the catalyst was cooled in $O_2$.

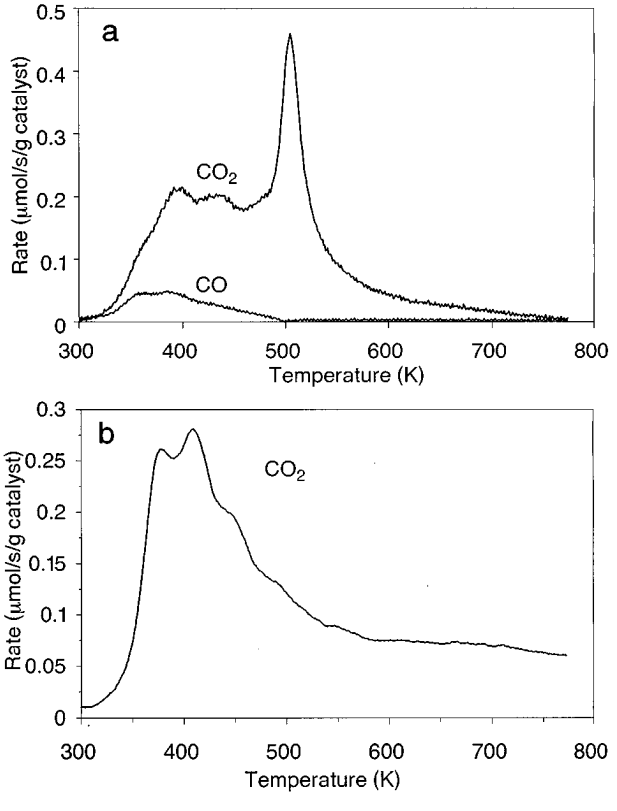


**FIG. 19.** Temperature-programmed desorption (a) and oxidation (b) spectra of CO adsorbed on $PdO/Al_2O_3$.

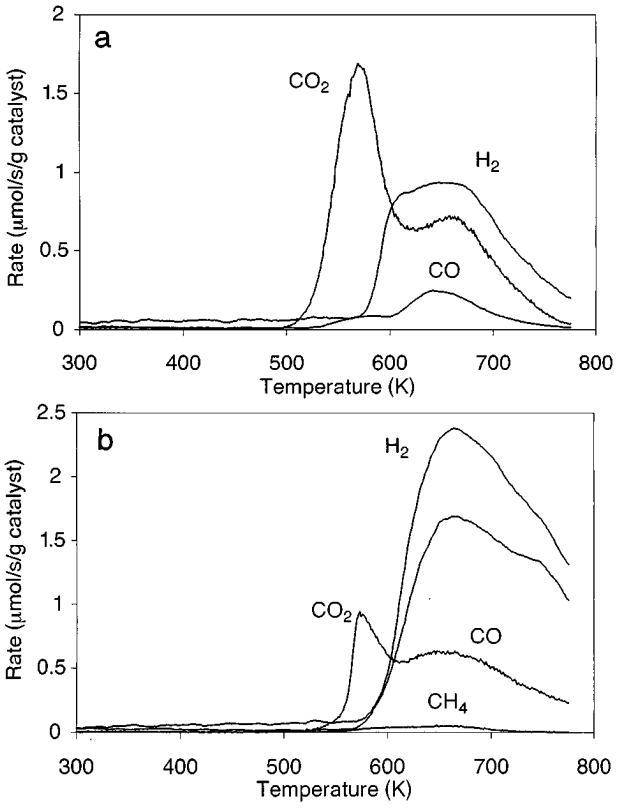


**FIG. 20.** Temperature-programmed desorption spectra after interrupted TPO of $CH_3OH$ (a) and $C_2H_5OH$ (b) up to 573 K on $Pd/Al_2O_3$.

## DISCUSSION

### *Decomposition of VOCs on $Al_2O_3$ and $Pd/Al_2O_3$*

Both dehydration and dehydrogenation of VOCs take place on the $Al_2O_3$ surface, and the reactions on $Al_2O_3$ provide a comparison to the reactions on $Pd/Al_2O_3$. Because methanol decomposes at such a high temperature (Fig. 1a), and because a fraction of the methanol injected into a blank reactor decomposed at 773 K, we were concerned that gas-phase decomposition might be contributing to the formation of CO and $H_2$ above 700 K. Matsushima and White (13) observed CO and $H_2$ from methanol on $Al_2O_3$ in UHV, however, showing that a surface reaction is responsible for their formation.

Even though the VOCs adsorb on the alumina support, the presence of palladium, which occupies a small fraction of the total surface area, significantly increases the rate of decomposition and changes the decomposition pathway more toward dehydrogenation. Both changes indicate that VOCs diffuse to and spill over onto the Pd surface to decompose. Since decomposition takes place at much lower temperatures for VOCs adsorbed on Pd metal (e.g., methanol dehydrogenates at 220 K on Pd(111) in UHV (14)), either diffusion or spillover must be limiting the rate of decomposition on $Pd/Al_2O_3$. Similar increases in rates

and shifts in reaction pathways have been observed for $Ni/Al_2O_3$ (8).

Methanol dehydrogenates on $Pd/Al_2O_3$ (Fig. 4a) with a peak temperature that is almost 300 K lower than that for $Al_2O_3$ (Fig. 1a). For a first-order process with a preexponential factor of $10^{13}$ $s^{-1}$, this corresponds to an increase in the rate of approximately $10^8$ (15). Desorption from the $Al_2O_3$ surface and readsorption on Pd is not responsible for the rate increase; methanol decomposition is almost complete by 600 K on $Pd/Al_2O_3$ (Fig. 4a), but the majority of methanol does not leave the $Al_2O_3$ surface, as decomposition products, until above 700 K (Fig. 1a). The rate of ethanol decomposition increases to a lesser extent, but mostly dehydrogenation takes place when Pd is present (Fig. 4b), whereas dehydration is the dominant reaction on $Al_2O_3$ (Fig. 1b). Formic acid and acetic acid also decompose faster on $Pd/Al_2O_3$, and dehydrogenation is the dominant reaction in each case. Formic acid decomposition produces mostly $CO_2$ and $H_2$, in agreement with the results obtained by Aas *et al.* (16) on Pd(110). Most of the acetic acid decomposes to CO and $H_2$ above 600 K on $Pd/Al_2O_3$ (Fig. 5b), whereas Aas *et al.* (17) observed that acetic acid decomposes to $CO_2$, $H_2$, and surface carbon near 353 K on Pd(111). Acetaldehyde decomposition also starts at a lower temperature in the presence of Pd, but acetaldehyde decomposes over a wide temperature range and decomposition is not complete by 773 K. Palladium has less of an effect on acetaldehyde decomposition.

In addition to decomposition on $Pd/Al_2O_3$, most of the VOCs decompose in parallel on $Al_2O_3$ to some extent. Dimethyl ether was not observed from methanol on $Pd/Al_2O_3$, apparently because much of the methanol decomposes at a lower temperature than that at which dimethyl ether forms. Since dimethyl ether forms mostly by reaction between two adsorbed methanol molecules (18), less dimethyl ether is expected at the lower methanol concentration. Products from decomposition on $Al_2O_3$ were observed on $Pd/Al_2O_3$, however, for ethanol, acetaldehyde, formic acid, and acetic acid since their decomposition rates in the presence of Pd increase less than does methanol decomposition. For each VOC, much less reaction occurs on the $Al_2O_3$ surface of $Pd/Al_2O_3$ than on $Al_2O_3$ alone, but the products appear in the same temperature range. For example, ethylene formation from dehydration of ethanol is suppressed on $Pd/Al_2O_3$ (Fig. 4b), but ethylene forms in the same temperature range as on $Al_2O_3$ (Fig. 1b). Acetaldehyde decomposition on $Pd/Al_2O_3$ forms $H_2$, CO, and $CO_2$ above 600 K, where these products also form from decomposition on $Al_2O_3$.

### *Oxidation of VOCs on $Al_2O_3$ and $Pd/Al_2O_3$*

Our TPO results show that $Al_2O_3$, which does not readily adsorb $O_2$, is not a good oxidation catalyst below 773 K. Instead, the VOCs decomposed before the $Al_2O_3$ reached a high enough temperature for oxidation, though some decomposition products were oxidized. For example, TPD and TPO spectra for formic acid on $Al_2O_3$ are identical and the CO product was not oxidized. Likewise, the TPD and TPO spectra for methanol (Figs. 1a and 9a) are similar, but because decomposition takes place above 700 K half of the $H_2$ product was oxidized to $H_2O$ and more $CO_2$ was formed. Similarly for ethanol, the $H_2$ product was oxidized to $H_2O$ and the ethylene product appeared to be oxidized to CO and $CO_2$. Some of the methanol oxidation may have taken place in the gas phase because of the high temperature; methanol injected into 3% $O_2$ flowing through a blank reactor at 773 K decomposed and 10% of the CO and 20% of the $H_2$ was oxidized. The products from TPO of acetaldehyde (Fig. 10) and acetic acid (Fig. 11) are the same as those formed during TPD on $Al_2O_3$ (Figs. 2 and 3b), and product evolution began at the same temperature in TPD and TPO, but the amounts of CO, $CO_2$, and $H_2O$ increased significantly.

The $Pd/Al_2O_3$ is a much more active catalyst for complete oxidation of VOCs than is $Al_2O_3$, as is shown by comparing Figs. 9a and 12 for methanol. The $CO_2$ product also started forming at a temperature 50 to 100 K lower during TPO than that at which CO or $CO_2$ formed during TPD on $Pd/Al_2O_3$, indicating that decomposition does not limit the oxidation rate. However, a much larger fraction of the carbon-containing products formed above 550 K during TPO than during TPD on $Pd/Al_2O_3$. Palladium starts to oxidize above 600 K during TPO (Fig. 18), and thus the $CO_2$ seen above 600 K forms on both Pd and PdO, as Pd and VOC oxidation take place simultaneously. The presence of $O_2$ did not increase the rate of product formation from formic acid and acetic acid on $Pd/Al_2O_3$, indicating that decomposition limits their oxidation. Parallel decomposition occurs on the $Al_2O_3$ surface since decomposition and oxidation were observed on $Al_2O_3$ in this temperature range.

For most VOCs, $CO_2$ was observed in two distinct temperature ranges during TPO on $Pd/Al_2O_3$ (e.g., Fig. 13). Apparently, part of the adsorbed VOC is oxidized completely and the rest forms a more stable, partial oxidation product, which oxidizes completely above 550 K. Temperature-programmed desorption following interrupted TPO (Fig. 20) shows that the species remaining on the surface after oxidation of alcohols to 573 K is a partially oxidized species. The $H/(CO + CO_2)$ ratio is much smaller than for the original alcohol. The products in Fig. 20 did not form at these high temperatures from decomposition of the original alcohol, which decomposed at lower temperatures (Fig. 4). Instead, the TPD spectra of ethanol after interrupted TPO are more like those seen for TPD of acetaldehyde and acetic acid (Fig. 4b), and thus one or both of these are likely the intermediate from partial oxidation

of ethanol. The TPD spectra of methanol after interrupted TPO is not like the TPD spectra of formic acid (Fig. 5a), however, and thus formaldehyde is a more likely intermediate for methanol oxidation.

The partial oxidation processes that form the more stable species are not a result of diffusion and spillover processes, but appear to take place on palladium. When the same VOCs were oxidized on $CuO/Al_2O_3$ by TPO, only one $CO_2$ peak formed and no evidence was seen for a partial oxidation product.

*Palladium Oxidation*

We observed an O/Pd ratio of 0.8 when our $Pd/Al_2O_3$ catalyst was oxidized between 600 and 773 K (Fig. 18). Note that this ratio does not include the $O_2$ that adsorbed rapidly and dissociatively upon exposure of the catalyst to $O_2$ at room temperature (18, 19). Since the palladium dispersion is 0.1–0.2, and the adsorbed oxygen could also oxidize the palladium, the total O/Pd ratio is 0.9–1.0. Briot and Primet (19) measured an O/Pd ratio of 1.05 during TPO on 1.95% $Pd/Al_2O_3$.

Paryjczak *et al*. (20), using pulse chromatography with Pd black, $Pd/Al_2O_3$, and $Pd/SiO_2$, postulated that oxygen is incorporated into Pd particles between 470 and 770 K by means of an activated mechanism in which adsorbed oxygen and surface metal atoms exchange places. They concluded that Pd oxidizes above 770 K, once the Pd lattice was saturated with oxygen. In contrast, Leon y Leon and Vannice (21), using chemisorption measurements on $Pd/SiO_2$, reported oxygen incorporation into the bulk above 300 K and bulk PdO formation at 473 K. Our results and the findings of Hoost and Otto (22) show oxidation at intermediate temperatures, perhaps indicating a dependence on particle size and support.

Hoost and Otto (22) performed TPO of $Pd/Al_2O_3$ with several Pd weight loadings using a heating rate of 0.25 K/s. For Pd weight loadings of 5 and 10%, $O_2$ was consumed in two uptake peaks at 623 and 873 K, and the O/Pd ratio was 1. The lower-temperature peak was attributed to bulk oxidation of Pd particles, and the higher-temperature peak to oxidation of Pd particles interacting strongly with $Al_2O_3$. Catalysts with 0.5 and 1% Pd had an O/Pd ratio significantly greater than one. They suggested that highly dispersed Pd may form an oxygen-rich Pd–$Al_2O_3$ species. The PdO did not decompose by 773 K, in agreement with previous studies that used similar Pd loadings (21, 23). Hoost and Otto (22) saw decomposition of PdO on $PdO/Al_2O_3$ above 1073 K, and Farrauto *et al*. (23) saw the same behavior between 1023 and 1073 K.

*Oxidation of VOCs on $PdO/Al_2O_3$*

The $PdO/Al_2O_3$ is a less active catalyst than $Pd/Al_2O_3$ for VOC decomposition. Lattice oxygen in PdO is extracted by VOCs, and thus much more $CO_2$ was observed at low temperature during TPD on PdO than on Pd (e.g., compare Figs. 4 and 6 for alcohols). The $CO_2$ and $H_2O$ began to form at similar temperatures during TPD of methanol, ethanol, and acetaldehyde on $PdO/Al_2O_3$ (Figs. 6 and 7). Water is concluded to form at the same temperature as $CO_2$ because $H_2$ formation was delayed relative to $CO_2$ and CO; the $H_2O$ forms and adsorbs on the $Al_2O_3$. Apparently extraction of lattice oxygen from PdO is the limiting step in the formation of decomposition products. As Pd sites become available due to removal of lattice oxygen, the VOCs decompose on the Pd in parallel with extraction of lattice oxygen. Hydrogen desorbs as Pd sites became available, but hydrogen is oxidized more readily than CO by lattice oxygen.

Temperature-programmed oxidation of VOCs is much slower on PdO than on Pd (e.g., compare Figs. 13 and 16). On $PdO/Al_2O_3$, oxidation during TPO and decomposition during TPD began at the same temperature; that is, oxygen extraction from the PdO lattice appears to be the first step for both TPD and TPO, and it determines the temperature at which $CO_2$ and $H_2O$ form. Since reaction products started forming between 400 and 450 K, but Pd was only oxidized above 600 K, Pd metal formed during TPO and TPD on $PdO/Al_2O_3$. These Pd sites catalyze VOC decomposition during TPD, and they provide sites for dissociative adsorption of $O_2$ during TPO. The increase in Pd sites with time increases the oxidation rate, and this autocatalytic effect causes the relatively narrow $CO_2$ peaks observed during oxidation of ethanol (Fig. 16a) and acetaldehyde (Fig. 16b). The Pd is reoxidized by gas-phase $O_2$ above 600 K, and thus the high-temperature $CO_2$ peaks in Figs. 15–17 form on Pd and PdO. Similar high-temperature $CO_2$ peaks were also seen during TPO when $Pd/Al_2O_3$ was the starting catalyst, and the oxidation process is probably the same at high temperatures. That is, VOCs most likely oxidize above 600 K through an oxidation-reduction cycle of the Pd particles (Mars–van Krevelen mechanism). Garbowski *et al*. (11) and Farrauto *et al*. (23) observed the same phenomena during $CH_4$ oxidation on $Pd/Al_2O_3$ at high temperature.

During TPO of acetic acid on $PdO/Al_2O_3$ (Fig. 17b), both $CO_2$ formation and Pd oxidation started near 600 K. Thus, much of the oxidation takes place on PdO, and $CO_2$ formation was quite similar whether PdO or Pd was the starting catalyst. There is a large difference between the TPD and TPO results for acetic acid on $PdO/Al_2O_3$; acetic acid oxidation is slower during TPO (Fig. 17b) than during TPD (Fig. 8b). The Pd sites created by extraction of lattice oxygen are more active during TPD; during TPO these sites are reoxidized to create a less reactive surface.

Farrauto *et al*. (23) found that $Pd/Al_2O_3$ is only active for $CH_4$ oxidation below 923 K because Pd does not adsorb $O_2$ above 923 K. The catalyst is active between 773 and 923 K when a mixture of Pd and PdO existed in the supported particles during steady-state operation because

the particles continued to adsorb $O_2$. Above 600 K, PdO is reduced by VOCs, and gas-phase $O_2$ reoxidizes the Pd. The VOCs are able to react with $PdO/Al_2O_3$, even though no adsorbed oxygen is present. Metallic Pd sites are necessary for oxygen to adsorb. Above 1073 K, Farrauto *et al*. (23) observed decomposition of PdO to Pd, which does not adsorb $O_2$ at that temperature. Reoxidation of Pd began only after the temperature was lowered below 923 K.

Others also reported that PdO is an active oxidation catalyst (11, 19, 24–30). Garbowski *et al*. (11) and Farrauto *et al*. (23) suggested that $CH_4$ oxidation on PdO at high temperatures followed a Mars–van Krevelen mechanism, in which $O_2$ chemisorbs and oxidizes surface Pd, which is then reduced by reaction when $CH_4$ adsorbs. Our results show directly that organics extract oxygen during TPO of VOCs above 600 K, the temperature at which Pd oxidation begins.

Oxygen reportedly reconstructs Pd particles. Several studies (11, 26, 29) proposed that activation of $Pd/Al_2O_3$ catalysts for $CH_4$ oxidation under an $O_2$ atmosphere is due to reconstruction. Palladium particles reconstruct by breaking large Pd particles into both PdO dispersed upon $Al_2O_3$ and large Pd particles with PdO on the metal surface. All of the PdO species are active in $CH_4$ oxidation, but the highly dispersed PdO is least active, possibly because of a strong interaction with the $Al_2O_3$ support.

### *Carbon Monoxide Oxidation*

Carbon monoxide oxidizes at room temperature on Pd, and the narrow $CO_2$ peak in Fig. 18 is indicative of an autocatalytic reaction such as that described on Pt by Ziff *et al*. (31). At the start of TPO, the surface is saturated with CO, which blocks sites for $O_2$ adsorption. Oxygen adsorption sites are created as CO is removed from the surface as $CO_2$, and the increased surface oxygen concentration accelerates the rate of oxidation. Previous studies have also found that CO readily oxidizes on Pd (32–37). On $PdO/Al_2O_3$, however, the CO oxidation rate is slower. An autocatalytic process does not appear to take place, and CO could only abstract lattice oxygen from PdO at higher temperature.

Note that CO oxidation is fast relative to oxidation of the VOCs so that CO products that form during TPO are expected to readily oxidize to $CO_2$ at the elevated temperatures where VOC decomposition occurs. Coadsorbed CO and methanol have little effect on their individual oxidation rates. Carbon monoxide is oxidized at low temperatures, and thus its rate of oxidation is not affected by methanol adsorbed on $Al_2O_3$. The presence of CO adsorbed on Pd slowed oxidation of methanol until 400 K because $O_2$ adsorption sites are blocked by CO. These results are independent of the order of adsorption since CO adsorbs on Pd and methanol adsorbs on $Al_2O_3$. Any methanol that adsorbs on Pd is apparently easily displaced by CO. The inhibition of methanol oxidation by CO was observed under steady-state conditions by Brewer *et al*. (38). According to their study, CO adsorbs on Pd until the CO oxidation rate becomes significant above 448 K, permitting adsorption of methanol at the same sites.

## CONCLUSIONS

Volatile organic compounds adsorbed on the $Al_2O_3$ support of $Pd/Al_2O_3$ decompose by surface diffusion to Pd sites. Reaction on Pd is mostly dehydrogenation and is much faster on Pd than on $Al_2O_3$. A fraction of the VOCs decompose on $Al_2O_3$ in a parallel reaction. Similarly, VOCs diffuse to Pd and react with adsorbed oxygen to form $CO_2$ and $H_2O$ at a much faster rate than on $Al_2O_3$. When VOCs are adsorbed on $PdO/Al_2O_3$, the lattice oxygen in PdO is reactive, and all the VOCs except acetic acid began reacting between 400 and 450 K, approximately 100 K higher than on $Pd/Al_2O_3$. Consumption of lattice oxygen creates metallic Pd sites, and decomposition of VOCs at these Pd sites takes place in parallel with oxidation, apparently because replenishment of surface oxygen from the bulk is slow. Hydrogen oxidizes to $H_2O$ more rapidly on PdO than carbon products oxidize to $CO_2$. Oxidation of VOCs begins at the same temperature on $PdO/Al_2O_3$ in the presence or absence of $O_2$, so extraction of lattice oxygen from PdO appears to be the limiting factor in the reaction. As lattice oxygen is consumed, Pd sites are generated for $O_2$ adsorption. Reaction with adsorbed oxygen is more rapid than with the lattice oxygen until above 600 K, where oxidation results are consistent with a Mars–van Krevelen mechanism because Pd oxidation is faster. Partial-oxidation products apparently form on the surfaces of both $Pd/Al_2O_3$ and $PdO/Al_2O_3$ and these products only oxidize at higher temperatures.

## ACKNOWLEDGMENTS

We gratefully acknowledge the partial support of National Science Foundation Grant CTS-90-21194. Acknowledgment is also made to the donors of the Petroleum Research Fund, administered by the American Chemical Society, for the partial support of this research.

## REFERENCES

1. Spivey, J. J., *Ind. Eng. Chem. Res.* **26**, 2165 (1987).
2. Falconer, J. L., and Schwarz, J. A., *Catal. Rev.-Sci. Eng.* **25**, 141 (1983).
3. Hsiao, E. C., and Falconer, J. L., *J. Catal.* **132**, 145 (1991).
4. Karski, S., *Przem. Chem.* **71**, 177 (1992).
5. Froment, G. F., and Bischoff, K. B., "Chemical Reactor Analysis and Design." Wiley, New York, 1990.
6. Hougen, O. A., *Ind. Eng. Chem.* **53**, 509 (1961).
7. Demmin, R. A., and Gorte, R. J., *J. Catal.* **90**, 32 (1984).
8. Chen, B., and Falconer, J. L., *J. Catal.* **144**, 214 (1993).
9. Swecker, J. L., and Datye, A. K., *J. Catal.* **121**, 196 (1990).
10. Cordi, E. M., and Falconer, J. L., *Catal. Lett.,* **38**, 45 (1996).
11. Garbowski, E., Feumi-Jantou, C., Mouaddib, N., and Primet, M., *Appl. Catal. A: General.* **109**, 277 (1994).
12. Albers, P., and Seibold, K., *J. Chem. Soc. Faraday Trans.* **82**, 3671 (1990).

13. Matsushima, T., and White, J. M., *J. Catal.* **44**, 183 (1976).
14. Kok, G. A., Noordermeer, A., and Nieuwenhuys, B. E., *Surf. Sci.* **135**, 65 (1983).
15. Falconer, J. L., and Madix, R. J., *Surf. Sci.* **48**, 393 (1975).
16. Aas, N., Li, Y., and Bowker, M., *J. Phys. Condens. Matter.* **3**, S281 (1991).
17. Aas, N., and Bowker, M., *J. Chem. Soc. Faraday Trans.* **89**, 1249 (1993).
18. Zwinkels, M. F. M., Järås, S. G., and Menon, P. G., *Catal. Rev. Sci. Eng.* **35**, 319 (1993).
19. Briot, P., and Primet, M., *Appl. Catal.* **68**, 301 (1991).
20. Paryjczak, T., Jozwiak, W. K., and Goralski, J., *J. Chromatogr.* **155**, 9 (1978).
21. Leon y Leon, C. A., and Vannice, M. A., *Appl. Catal.* **69**, 269 (1991).
22. Hoost, T. E., and Otto, K., *Appl. Catal. A: General* **92**, 39 (1992).
23. Farrauto, R. J., Hobson, M. C., Kennelly, T., and Waterman, E. M., *Appl. Catal.* **81**, 227 (1992).
24. Jones, M. G., and Nevell, T. G., *J. Catal.* **122**, 219 (1990).
25. Jones, M. G., and Nevell, T. G., *Appl. Catal.* **70**, 277 (1991).
26. Baldwin, T. R., and Burch, R., *Appl. Catal.* **66**, 337 (1990).
27. Baldwin, T. R., and Burch, R., *Appl. Catal.* **66**, 359 (1990).
28. Hicks, R. F., Qi, H., Young, M. L., and Lee, R. G., *J. Catal.* **122**, 280 (1990).
29. Hicks, R. F., Qi, H., Young, M. L., and Lee, R. G., *J. Catal.* **122**, 295 (1990).
30. Ribeiro, F. H., Chow, M., and Dalla Betta, R. A., *J. Catal.* **146**, 537 (1994).
31. Ziff, R. M., Gulari, E., and Barshad, Y., *Phys. Rev. Lett.* **56**, 2553 (1986).
32. Choi, K. I., and Vannice, M. A., *J. Catal.* **131**, 1 (1991).
33. Ehsasi, M., Berdau, M., Rebitzki, T., Charlé, K. P., Christmann, K., and Block, J. H., *J. Chem. Phys.* **98**, 9177 (1993).
34. Ladas, S., Imbihl, R., and Ertl, G., *Surf. Sci.* **280**, 14 (1993).
35. Szanyi, J., and Goodman, D. W., *J. Phys. Chem.* **98**, 2972 (1994).
36. Szanyi, J., Kuhn, W. K., and Goodman, D. W., *J. Phys. Chem.* **98**, 2978 (1994).
37. Valden, M., Aaltonen, J., Kuusisto, E., Pessa, M., and Barnes, C. J., *Surf. Sci.* **307–309**, 193 (1994).
38. Brewer, T. F., and Abraham, M. A., *Ind. Eng. Chem. Res.* **33**, 526 (1994).